The 2009 IEEE/RSJ International Conference on
Intelligent Robots and Systems
October 11-15, 2009 St. Louis, USA

Mobile Manipulation Using Tracks of a Tracked Mobile Robot

Yugang Liu and Guangjun Liu*, *Senior Member, IEEE*

Abstract— **This paper presents the investigation on mobile manipulation of a self-reconfigurable tracked mobile robot, using its tracks for both manipulation and locomotion. It is desirable for a mobile robot to possess manipulation capability in unstructured environments, especially in the scenario which is unsuitable for human beings. However, it is not convenient for such a mobile robot to carry an onboard manipulator and perform grasping and placing operations. An alternative is to realize the manipulation potential of the existing parts and perform manipulation without attaching additional hardware. Besides the enhanced locomotion ability, a self-reconfigurable tracked mobile robot has great potential in manipulation, which may take the forms of box-pushing, cylinder-moving or lateral hitting. However, the manipulation with tracks has to be controlled properly. One challenge is to optimize the tracks' configuration so as to get the optimal contact point. Furthermore, the speed and acceleration of the mobile robot have dramatic influence on mobile manipulation with tracks. To verify the effectiveness of the proposed algorithms, experiments are conducted using a tracked mobile robot in our laboratory.**

I. INTRODUCTION

Tracked mobile robots are gaining increasing attention since they normally provide better floatation and traction than wheeled ones due to larger contact area with the terrain, and this characteristic brings them substantial application potentials in rescuing, searching, explosive ordnance disposing, mining, logging, farming, earth moving, and planetary exploring among others. Tracked mobile robots possess extraordinary locomotion capabilities, such as climbing stairs, surpassing obstacles or negotiating irregular terrain. However, their great potential in manipulation has not been paid much research attention. In this paper, we investigate the manipulation of various objects with a self-reconfigurable tracked mobile robot using its tracks.

Manipulation is a well documented research topic in robotic manipulators. With the development of mobile robot technology, the concept of manipulation has been extended to mobile manipulation, which involves the robot locomotion and manipulation of objects, i.e., moving some collective of objects relative to the robot [1]. A direct approach for mobile manipulation is to attach an onboard manipulator, while the mobile robot is employed to carry the manipulator for locomotion purpose [2]. Other solutions involve attaching a simple gripper to the mobile robot and manipulating the object with multiple agents [3], or integrating both manipulation and locomotion into one entry [1], [4].

Manuscript received March 1, 2009. This work was supported in part by the Canada Research Chair Program and in part by the Natural Sciences and Engineering Research Council (NSERC) of Canada.

The authors are with Department of Aerospace Engineering, Ryerson University, 350 Victoria St., Toronto, Ontario Canada M5B 2K3.

*The corresponding author (E-mail: gjliu@ryerson.ca).

In related research on mobile manipulation, a mobile robot called "Mobipulator" was designed to locomote and simultaneously manipulate objects on a desktop in [1], which combines locomotion and manipulation elegantly with the wheels. Path following control was investigated for a redundant nonholonomic mobile manipulator with consideration of tip-over stability [2]. A tracked mobile manipulator was designed in [4], using the manipulator for either locomotion or manipulation. Nonholonomic mobile robots have demonstrated extensive potential for box-pushing operations in structured environments [5]. A whole body postural control algorithm was developed to optimize the manipulation forces applied to the environment for pushing, pulling or carrying types of tasks [7]. With the advent of light-weight tracked mobile robots, tip-over stability analysis as well as tip-over prediction for stair-climbing tracked mobile robots have been paid much attention [8], [9].

Attaching an onboard manipulator may not suit for many tracked mobile robots due to the complex vehicle-manipulator interactions [10] and the difficulties in their coordination [11]. Carrying an onboard manipulator upstairs or through an irregular terrain itself may become a burden to the mobile robot [9]. Furthermore, grasping operation for a mobile manipulator in unstructured environments is challenging, and the payload capability for such an integrated structure is quite limited, as the onboard manipulator has to be relatively light to avoid tipping over and other problems. In addition, it is difficult to design a universal gripper that fits all potential objects with various shapes and dimensions.

In this paper, we study the manipulation capability of a tracked mobile robot with its existing parts. According to the shape and dimension of the objects to be manipulated, the manipulation can take the forms of box-pushing, cylinder-moving or lateral hitting. Sufficient and necessary conditions for stable pushing are derived for box-pushing without tumbling. Furthermore, an algorithm is proposed to optimize the pushing point by adjusting the configuration of the robot. For the cylinder-rolling mode, the conditions for successful rolling are derived and the procedure for rolling cylinders is presented. Lateral hitting suits for low objects, which cannot be manipulated with cylinder-moving mode or box-pushing mode. However, lateral hitting mode does not suit for manipulation of heavy objects, and the motion of the object as well as the hitting force are difficult to determine.

The rest of this paper is organized as follows: a tracked mobile robot used in this study is introduced and various manipulation modes are analyzed systematically for the robot in Section II. Experimental results are presented in Section III. Some concluding remarks are given in the last section.

II. Modeling and Analysis for Mobile Manipulation with Tracks

In this section, the self-reconfigurable tracked mobile robot under investigation is introduced, and mobile manipulation is modeled and analyzed for various manipulation modes.

A. A Self-reconfigurable Tracked Mobile Robot

The self-reconfigurable tracked mobile robot used in this investigation is RLMA, a customized product of Engineering Service Inc. (ESI) [13]. The RLMA consists of a chassis, two tracks, two driving wheels, two supporting wheels and two planetary wheels, as shown in Fig. 1. The two driving wheels can be controlled independently to realize steering; the two planetary wheels are attached at the tip of the flippers; and the two flippers, which are installed at the flanks of the chassis, are driven by one motor (pitch motor) to ensure synchronization of the two tracks. To retain tension in each track, the flippers are equipped with spring loaded prismatic joints, as shown in Fig. 1(d). The tracks are equipped with grousers, which helps strengthen the locomotion and manipulation capabilities of the robot in unstructured environments, as shown in Fig. 1. According to the motion of the pitch joint, as well as the position of the flippers and planetary wheels, the RLMA may take four different configurations, as shown in Figs. 1(a)–(d).

For the RLMA, three drives are dedicated to control the motors and a PC-104 board running QNX is used for high-level control. A three-axis compass is equipped to measure the pitch, roll and yaw of the chassis. Cameras are installed at the front and the back of chassis, as shown in Fig. 1. The communication between the drives and PC-104 is through CAN bus. An operator control unit (OCU) sends control command to and collect sensor information from the RLMA. The communication between the OCU and the RLMA is via radio frequency transmitters and data modems.

Though not designed specially for manipulation purpose, the RLMA exhibits excellent manipulation performance and can be used for moving objects occasionally in unstructured or hostile environments.

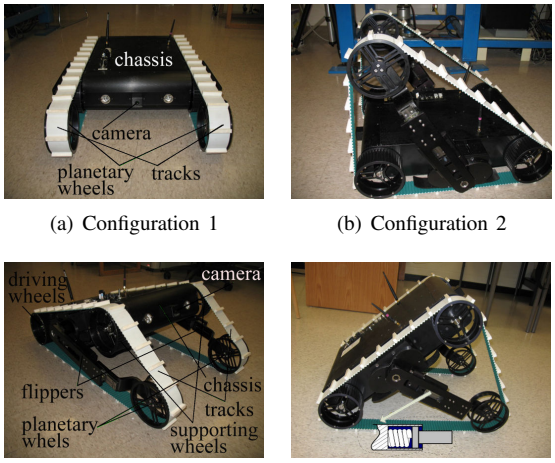

(a) Configuration 1 (b) Configuration 2

(c) Configuration 3 (d) Configuration 4

Fig. 1. A self-reconfigurable tracked mobile robot RLMA

B. Box-pushing Mode Analysis

In this subsection, the sufficient and necessary stable pushing conditions are derived, which can ensure the objects being pushed without tumbling. Furthermore, an algorithm is developed to adjust the pushing point by reconfiguring the mobile robots.

Intuitively, the object may tumble backward around point A in Fig. 2(a), if a narrow and high object is pushed; similarly, the object may be pushed down and falling forward around point B in Fig. 2(b).

To simplify the calculations, the object is assumed to be a symmetrical box-like rigid object, with the width b and height h, as shown in Fig. 2. The sinkage of the tracks is assumed to be negligible, and the object is assumed to be pushed following a line, i.e., the lateral slippage is assumed to be zero. The normal forces under the tracks are assumed to have the form of trapezoid. Then, the tractive forces and the external motion resistance between the tracks and the terrain can be calculated by, [12]

$$\begin{aligned} F &= 2B\int_{-\frac{L}{2}}^{L_c-\frac{L}{2}} \mu_1 p(x)\left[1-\exp\left(-\tfrac{j}{K_1}\right)\right]dx \\ R &= 2B\int_{-\frac{L}{2}}^{L_c-\frac{L}{2}} f_{r1}p(x)dx \end{aligned} \tag{1}$$

where p is the normal pressure on the tracks exerted by the terrain; μ_1 and f_{r1} are the coefficients of friction and external motion resistance, respectively; B denotes the width of the tracks; and L_c is length of the tracks contacting with the terrain, which equals $\frac{L}{2}+L_{p0}$ in *Cfg. 1* and L in *Cfg. 2* (*Cfg* is the abbreviation of *Configuration*); K is shear deformation modulus between the tracks and the terrain; and j represents the corresponding shear displacement.

In the same way, the track-object interactive forces in Figs. 2(a)-(b), can be calculated as follows

$$\begin{aligned} F_{ro} &= \mu_2 N_{ro}\left[1-exp\left(-\tfrac{j}{K_2}\right)\right] \\ R_{ro} &= f_{r2}N_{ro} \end{aligned} \tag{2}$$

where N_{ro}, F_{ro}, R_{ro} represent the normal force, tractive force and external motion resistance exerted to the robot by the object; μ_1 and f_{r1} are the coefficients of friction and external motion resistance between the tracks and the object.

To simplify the calculations, the normal force generated at the object-terrain contact area is simplified to points A and B, as shown in Fig. 2(b), and the frictional forces can be calculated by

$$F_A = \mu_3 N_A, \qquad F_B = \mu_3 N_B \tag{3}$$

where μ_3 is the coefficient of friction between the object and the terrain.

According to Newton's third law of motion, the forces applied to the object by the track equal to those the track received from the object. In Fig. 2(b), the summation of forces along O_mX_m applied to the object being zero yields

$$N_{ro} - m_o a_o - \mu_3(N_A + N_B) = 0 \tag{4}$$

where m_o is the mass of the object; a_o is the acceleration of the object; N_A, N_B represent normal forces applied to the object at the points 'A' and 'B', respectively.

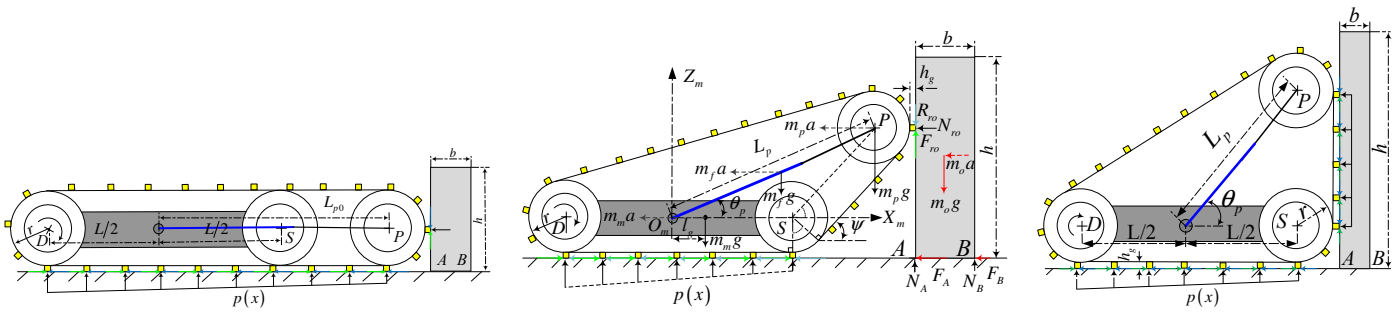

(a) Pushing with Cfg 1 (b) Pushing with Cfg 2: one point (c) Pushing with Cfg 2: multiple points

Fig. 2. Box-pushing mode analysis

In Fig. 2(b), the summation of forces along O_mZ_m applied to the object being zero yields

$$(N_A + N_B) - m_o g - k_p N_{ro} = 0 \tag{5}$$

where $g = 9.81m/s^2$ is the gravitational acceleration; and $k_p = \mu_2 \{1 - \exp(-j/K_2)\} - f_{r2}$.

In Fig. 2(b), let the summation of moments about the line passing through point A and parallel to O_mY_m be zero, we can obtain

$$N_B b + m_o a_o \tfrac{h}{2} - m_o g \tfrac{b}{2} - N_{ro}(z_P + h_g + r) = 0 \tag{6}$$

where z_p is the vertical coordinate of the pushing point with respect to frame $O_m - X_mY_mZ_m$, as shown in Fig. 2(b).

Solving the equation group (4)-(6) yields

$$\begin{aligned} N_A &= \left(k_p - \tfrac{z_P+h_g+r}{b}\right)N_{ro} + m_o\left(\tfrac{h}{2b}a_o + \tfrac{1}{2}g\right) \quad (a)\\ N_B &= \left(\tfrac{z_P+h_g+r}{b}\right)N_{ro} - m_o\left(\tfrac{h}{2b}a_o - \tfrac{1}{2}g\right) \quad (b)\\ N_{ro}(1-\mu_3 k_p) &= m_o(a_o + \mu_3 g) \quad (c) \end{aligned} \tag{7}$$

The terrain generates unilateral constraints, i.e., it can only provide supporting force to prevent the object plunging into the terrain but cannot provide pulling force to prevent it from leaving the terrain. Assuming that the calculated normal force N_A, which is necessary to construct a force-balanced system, is negative in Fig. 2(b), the object will rotate around point B and tumble forward. Similarly, with the assumption that the required supporting force N_B is negative, the object will tumble backward. From the above analysis, the sufficient and necessary condition for stable pushing can be derived from (7) as follows:

$$\begin{aligned} &\left(\tfrac{h}{2}a_o - \tfrac{b}{2}g\right)\left(\tfrac{1-\mu_3 k_p}{a_o+\mu_3 g}\right) \le z_p + h_g + r \\ &\le k_p b + \left(\tfrac{h}{2}a_o + \tfrac{b}{2}g\right)\left(\tfrac{1-\mu_3 k_p}{a+\mu_3 g}\right) \end{aligned} \tag{8}$$

Remark 1: The left side of (8) gives the sufficient and necessary condition for the object not tumbling backward. Since $\mu_3 k_p < 1$ for most terrain, as long as $a_o < \frac{b}{h}g$, this condition will always hold, and the object will not tumble backward. This remark explains why the object with bigger height/width ratio is easier to tumble backward. Similarly, the right side of (8) gives the reason why the object is easy to tumble forward with a high pushing point.

Let D, S, P represent points on the axes of driving wheels, supporting wheels, and planetary wheels. With the assumption that the tracks' length can be retained, from Fig. 2, the trajectory of P is an ellipse with D, S as the foci, which can be determined by the following equation:

$$\frac{x_p^2}{L_p^2(0)} + \frac{z_p^2}{L_p^2\left(\frac{\pi}{2}\right)} = 1 \tag{9}$$

where $L_p(0), L_p\left(\frac{\pi}{2}\right)$ represent the length of the flippers at the horizontal and vertical positions, respectively, which are constants and can be determined from the wheel radius r and the track length L_t as follows:

$$\begin{aligned} L_p(0) &= \tfrac{L_t}{2} - \tfrac{L}{2} - \pi r \\ L_p\left(\tfrac{\pi}{2}\right) &= \tfrac{\sqrt{(L_t - 2\pi r - 2L)(L_t - 2\pi r)}}{2} \end{aligned} \tag{10}$$

Since $x_p = L_p(\theta_p)\cos\theta_p$ and $z_p = L_p(\theta_p)\sin\theta_p$, as shown in Fig. 2(b), substituting this result into (9) yields

$$L_p(\theta_p) = \frac{L_p(0)\, L_p\left(\frac{\pi}{2}\right)}{\sqrt{L_p^2\left(\frac{\pi}{2}\right)\cos^2\theta_p + L_p^2(0)\sin^2\theta_p}} \tag{11}$$

Substituting (11) into $z_p = L_p(\theta_p)\sin\theta_p$ and then the result into (8), we can obtain the sufficient and necessary pushing conditions expressed by θ_p. Furthermore, the range of θ_p can be determined by solving the resulted inequality equation, which will not be detailed here.

With the assumption that the normal forces under the tracks have the forms of trapezoid, we can obtain the pressure shown in Fig. 2(b), as follows:

$$\begin{aligned} p(x) = &\tfrac{1}{2BL}\{(m_m + 2m_f + 2m_p)g - k_p N_{ro}\} \\ &+ \tfrac{6x\{m_m L_g g - 2(m_f L_f + m_p L_p)(a_r \sin\theta_p - g\cos\theta_p)\}}{BL^3} \\ &- \tfrac{6x\{N_{ro}[L_p\sin\theta_p + k_p(L_p\cos\theta_p + r + h_g)]\}}{BL^3} \end{aligned} \tag{12}$$

where a_r is acceleration of the robot.

Substituting (12) into (1)-(2) yields

$$F - R = k\{(m_m + 2m_f + 2m_p)g - k_p N_{ro}\} \tag{13}$$

where $k = \mu_1\{1 - \exp(-j/K_1)\} - f_{r1}$.

In Fig. 2(b), letting the summation of forces applied to the robot along O_mX_m be zero yields

$$F - R - N_{ro} - (m_m + 2m_f + 2m_p)a_r = 0 \tag{14}$$

Substituting (13) into (14) yields

$$N_{ro} = \tfrac{(m_m + 2m_f + 2m_p)(kg - a_r)}{1 + kk_p} \tag{15}$$

With the assumption that the object will not tumble over, the object and the robot will have the same acceleration during the course of steady-pushing (except for the starting and stopping phases), i.e., $a_r = a_o = a$. Substituting (15) into (7c), we can obtain

$$a = \frac{(m_m+2m_f+2m_p)(1-\mu_3 k_p)k - m_o(1+kk_p)\mu_3}{(m_m+2m_f+2m_p)(1-\mu_3 k_p)+m_o(1+kk_p)} g \tag{16}$$

To push the object successfully, the assumed acceleration should be non-negative, otherwise the robot cannot provide enough tractive forces and the pushing operation may stop without being finished. Therefore, the maximum mass of the object that the robot can push will be determined by

$$m_o \leq \frac{(m_m+2m_f+2m_p)(1-\mu_3 k_p)k}{(1+kk_p)\mu_3} \tag{17}$$

Remark 2: In this section, we present three cases of box-pushing manipulation, as shown in Fig.2. The one shown in Fig. 2(a) can be viewed as a special case of that shown in Fig. 2(b) with $\theta_p = 0$. The former may provide larger pushing force due to larger contact area, and its problem lies in that the object being pushed may tumble down backward, especially for those with big height/width ratios. The latter is preferred because it can adjust pushing point intelligently; however, it also raises the possibility of pushing the object down forward. Comparing to the aforementioned two cases, the multiple point pushing case shown in Fig. 2(c) may provide the best stability, because it increases the number of supporting points. However, the possibility of scratching the object is increased due to the increased contact area with the object. Another concern is that the camera may be damaged when interacting with the object in Fig. 2(c).

C. Cylinder-moving Mode Analysis

Noble dung beetles are experts in manipulating ball-like or cylindrical objects, which can be several times heavier than their weight. Dung beetles sometimes roll a large sphere object on top of it. Inspired by this observation, we can control the robot to climb onto a cylinder to pull it with the aid of the robot's own weight. In this subsection, the cylinder-moving mode is divided into cylinder-pulling and cylinder-pushing mode. The necessary condition for successful pushing is derived and the procedure for cylinder-pulling mode is presented.

In Fig. 3, letting the summation of forces exerted on the object along $O_m X_m$ be zero yields,

$$F_{or}\sin\theta + N_{or}\cos\theta - m_o a_o - F_o = 0 \tag{18}$$

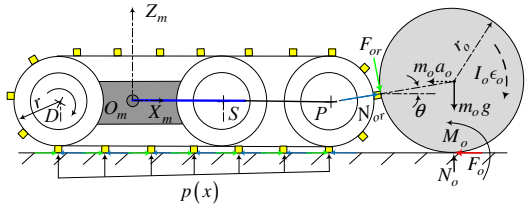

Fig. 3. Cylinder pushing mode analysis

where $\theta = \arcsin\{(r_o - r - h_g)/(r + r_o + h_g)\}$.

Also in Fig. 3, if the summation of forces applied to the object along $O_m Z_m$ is zero, we have

$$N_{or}\sin\theta - F_{or}\cos\theta + N_o - m_o g = 0 \tag{19}$$

Similarly, letting the summation of moments exerted on the object around the axis of the cylinder be zero yields,

$$M_o = (F_o - F_{or})\, r_o + I_o\epsilon_o \tag{20}$$

where m_o and I_o are the mass and inertial moment of the object, respectively; a_o and ϵ_o are the linear and angular accelerations of the object; F_o and M_o represent the sliding and rolling friction between the object and the terrain. In the steady state of cylinder moving, the accelerations should all be zeroes, i.e., $a_o = \epsilon_o = 0$; then from (18)-(20),

$$\begin{aligned} F_o &= F_{or}\sin\theta + N_{or}\cos\theta && (a)\\ N_o &= m_o g - N_{or}\sin\theta + F_{or}\cos\theta && (b)\\ M_o &= (F_{or}\sin\theta + N_{or}\cos\theta - F_{or})\, r_o && (c) \end{aligned} \tag{21}$$

Let δ_{max}, μ_{max} be the coefficients for maximum static rolling friction and maximum static sliding friction between the object and the terrain, respectively; then the motion of the cylinder can be categorized into the following cases:

Case 1: If $\{M_o < -\delta_{max}N_o\} \cap \{F_o \leq \mu_{max}N_o\}$, the cylinder will roll counter-clockwise without sliding;

Case 2: If $\{|M_o| \leq \delta_{max}N_o\} \cap \{F_o \leq \mu_{max}N_o\}$, the cylinder will keep static without rolling or sliding;

Case 3: If $\{M_o > \delta_{max}N_o\} \cap \{F_o \leq \mu_{max}N_o\}$, the cylinder will roll clockwise without sliding;

Case 4: If $\{M_o < -\delta_{max}N_o\} \cap \{F_o > \mu_{max}N_o\}$, the cylinder will roll counter-clockwise and slide forward;

Case 5: If $\{|M_o| \leq \delta_{max}N_o\} \cap \{F_o > \mu_{max}N_o\}$, the cylinder will slide forward without rolling;

Case 6: If $\{M_o > \delta_{max}\} \cap \{F_o > \mu_{max}N_o\}$, the cylinder will roll clockwise and slide forward.

Remark 3: In *Cases 3–6*, the cylinder can be manipulated successfully forward and *Case 6* provides the most effective manipulation because both rolling and sliding are in the preferred direction. On the other hand, the robot cannot manipulate the cylinder in *Cases 1–2* because it will keep static or rolling at the original position. From (21), the pushing force is affected by θ besides the weight of the object $m_o g$. Changing the robot's configuration so as to adjust the pushing point and pushing direction may help manipulate the cylinder in *Cases 1–2*; furthermore, the robot may pull the cylinder by climbing onto it, so that the weight can be used as active force to improve the pulling capability.

The procedure for cylinder-pulling mode can be given by:

Step 1: Driving the robot to the front (the desired manipulation direction) of the cylinder, raising its flippers and planetary wheels by adjusting configuration of the robot, and driving the robot to access the cylinder, as shown in Fig. 4(a);

Step 2: Driving the robot to climb onto the cylinder, until the pitch angle, which can be read from the 3-axis compass equipped inside the chassis, reaches a definite angle (e.g. 40°), as shown in Fig. 4(b);

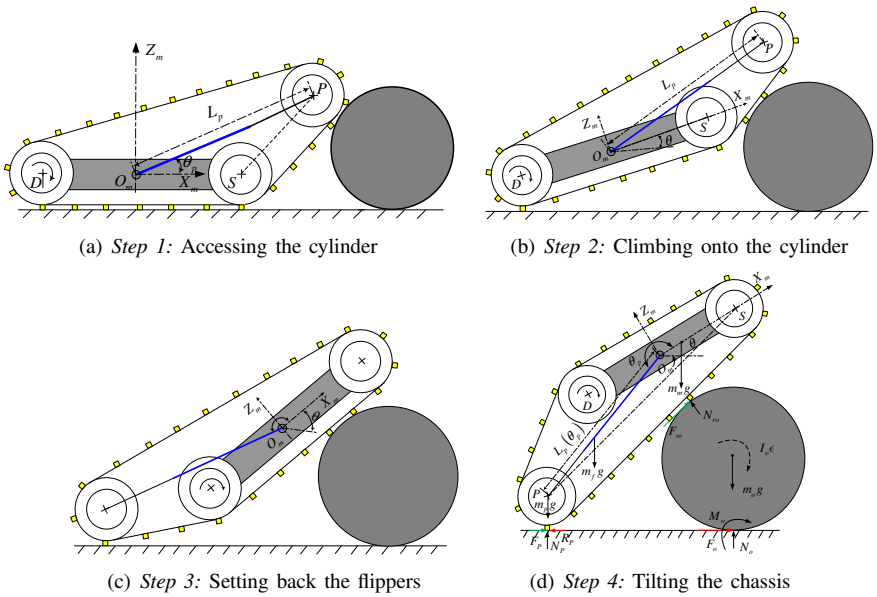

(a) *Step 1:* Accessing the cylinder

(b) *Step 2:* Climbing onto the cylinder

(c) *Step 3:* Setting back the flippers

(d) *Step 4:* Tilting the chassis

Fig. 4. Procedure for cylinder pulling mode

Step 3: Setting the flippers and planetary wheels to put the COG of the robot forward, so as to increase the pulling force, as shown in Fig. 4(c);

Step 4: Driving the robot to climb onto the cylinder again with the flippers in the back, and the rotating the chassis clockwise, so as to increase the normal force exerted to the cylinder and to avoid colliding between the robot and the cylinder, as shown in Fig. 4(d).

The motion of cylinder-pulling mode is complex, which involves switching between "rolling the cylinder with the tracks" and "pushing the robot to move in the desired direction". Since the deformation of tracks is almost unavoidable when negotiating the surface of a cylinder, the force analysis becomes an intractable task. In this paper, the motion and forces for the self-reconfigurable tracked mobile robot pulling cylinders will not be detailed.

Remark 4: Since the tracks are equipped with grousers, the box-pushing mode and cylinder-moving mode do not suit for low objects, whose height is smaller than the wheel radius of the mobile robot. Otherwise, the robot will climb onto the object, in the same way as surpassing obstacles. To manipulate such a low object, the robot can hit it using the tracks and flippers by rotating around the vertical axis. Comparing to the box-pushing mode and the cylinder-moving mode, lateral hitting mode cannot be used to manipulate heavy objects, which may damage the tracks. Furthermore, it is almost impossible to control the motion of the object and the hitting force is difficult to determine, because lateral slippage is introduced besides the longitudinal one.

III. Experiments

To demonstrate the applications of the proposed algorithms, experiments are conducted on the RLMA. The design parameters of the RLMA are listed in Table I.

To investigate the influence of the object's height/width ratio, the pushing points, as well as accelerations to the object's tip-over stability in box-pushing mode, the RLMA is controlled to push boxes for four different cases, and the experimental setup is shown in Table II. The box is pushed successfully from the start line to the end line in *Case 1* and *Case 4*, as shown in Figs. 5(a) and (d), respectively; while the box tumbles down backward in *Case 2*, as shown in Fig. 5(b), and forward in *Case 3*, as shown in Fig. 5(c). All the phenomena can be observed from the attached video.

From the experiments, we can see that the possibility of tumbling increase dramatically with the increase of height/width ratio of the box to be pushed; with a low pushing point, the box may tumble backward; on the other hand, high pushing point may lead to tumbling forward. It is also observed from the experiments that the tracks may help recover stability of the box, i.e., even though its back border leaves the ground, the box can still be pushed successfully as required, as shown in *Case 4*. We also notice that oscillations of the box increase with the increase of pushing speed. Furthermore, if the robot start right in front of the box, i.e., it is accelerated together with the box, the possibility of tumbling will be reduced.

To study the cylinder-pushing mode, the RLMA is controlled to push a cylindrical bucket with different fillings on a carpet, as shown in Figs. 6(a)-(b). A *6-kg* empty bucket

TABLE I
Design Parameters and Terrain Parameters

Parameters	Values	Parameters	Values
$m_m(kg)$	42	$L\ (m)$	0.514
$m_p\ (kg)$	1.4	$L_t(m)$	2.046
$m_f\ (kg)$	2.0	$h_g(m)$	0.010
$L_g\ (m)$	0.2	$r\ (m)$	0.100

TABLE II

EXPERIMENTAL SETUP FOR BOX-PUSHING MODE

Cases	Height/width ratio	Pushing point height	Initial velocities
1	8	$0.11(m)$	$0.2(m/s)$
2	10	$0.11(m)$	$0.6(m/s)$
3	8	$0.25(m)$	$0.4(m/s)$
4	4	$0.40(m)$	$0.6(m/s)$

is pushed with two different speeds with *Cfg. 1*. And then the experiments are repeated by filling the bucket with *10-kg* and *20-kg* objects. It is observed from the experiments that the empty bucket moves in the manner of rolling without sliding; the bucket with *20-kg* fillings exhibits sliding without rolling; and the one with *10-kg* fillings has both rolling and sliding. It is also observed that the chassis is tilted when pushing the bucket with 20-kg fillings with *Cfg. 2*, as shown in Fig. 6(b). The RLMA is controlled to pull a E-sized empty oxygen cylinder off a carpet to demonstrate the cylinder-rolling mode, as shown in Figs. 6(e)-(h). Experiments for cylinder-moving mode is also shown in the attached video.

Lateral hitting mode is also tested with the RLMA. However, the experimental results are not satisfactory because the RLMA can not provide large hitting force. Furthermore, rotation around the vertical axis is not a preferred motion for tracked mobile robots because the lateral traction waste quantities of energy. In addition, the detracking problem may occur when rotating at high speeds.

To further investigate the manipulation potentials, the RLMA is controlled to push the aforementioned bucket with 20-kg fillings over an obstacle, as shown in Fig. 6(c). Furthermore, the RLMA has also exhibited excellent performance for pushing a four-wheeled cart, as shown in Fig. 6(d).

IV. CONCLUSIONS AND FUTURE WORKS

In this paper, the manipulation capability of a self-reconfigurable tracked mobile robot is investigated, using the tracks not only for locomotion, but also for manipulation. According to the shape and dimension of the objects to be manipulated, the manipulation may typically take three different modes in terms of box-pushing, cylinder-moving and lateral hitting modes. Sufficient and necessary stable pushing conditions are derived, which ensure that the object can be pushed without tumbling. The conditions for successfully pushing cylinders are also derived and the procedure for cylinder-pulling manipulation is presented. The effectiveness of some of the proposed algorithms is verified by experiments.

For the tele-operated mobile manipulation, the study in this paper can help a remote operator to select the suitable manipulation mode, manipulation speed as well as optimal configuration of the tracked mobile robots. Furthermore, this paper lays a solid foundation for autonomous or semi-autonomous mobile manipulation, which is also determined by the progress in such fields as automatic shape and dimension identification, as well as terrain characteristic extraction. With these problems resolved, an intelligent manipulation algorithm can be developed on the basis of the efforts made in this paper, which can direct the tracked mobile robot to manipulate the objects in unstructured environments with little and even no human being interference.

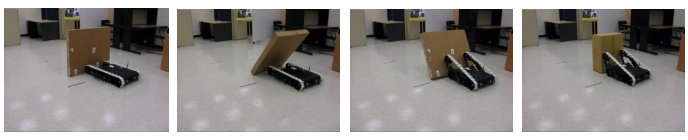

(a) *Case 1* (b) *Case 2* (c) *Case 3* (d) *Case 4*

Fig. 5. Snapshots for the RLMA pushing boxes

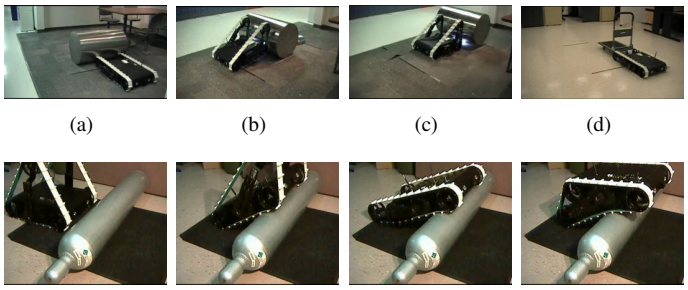

(a) (b) (c) (d) (e) (f) (g) (h)

Fig. 6. Snapshots for the RLMA moving cylinders and pushing a cart

REFERENCES

[1] M. T. Mason, D. K. Pai, D. Rus, L. R. Taylor, and M. A. Erdmann, "A mobile manipulator," in *Proc. IEEE Int. Conf. on Robotics and Automation*, Detroit, MI, USA, May 1999, pp. 2322–2327.

[2] Y. Li and Y. Liu, "Real-time tip-over prevention and path following control for redundant nonholonomic mobile modular manipulators via fuzzy and neural-fuzzy approaches," *ASME Trans. on Dynam. Syst., Measur., and Contr.*, vol. 128, no. 4, pp. 753–764, Dec. 2006.

[3] J. Spletzer, A. K. Das, R. Fierro, C. J. Taylor, V. Kumar, and J. P. Ostrowski, "Cooperative localization and control for multi-robot manipulation," in *Proc. IEEE/RSJ Intl. Conf. on Intelligent Robotics and Syst.*, Maui, HI, USA, Oct. 2001, pp. 631–636.

[4] P. Ben-Tzvi, A. A. Goldenberg, and J. W. Zu, "Design, simulations and optimization of a tracked mobile robot manipulator with hybrid locomotion and manipulation capabilities," in *Proc. of IEEE Int. Conf. on Robotics and Automation*, Pasadena, CA, USA, May 2008, pp. 2307–2312.

[5] R. Emery and T. Balch, "Behavior-based control of a non-holonomic robot in pushing tasks," in *Proc. of IEEE Intl. Conf. on Robotics and Autonomation*, Seoul, Koera, May 2001, pp. 2381–2388.

[6] Y. Okawa and K. Yokoyama, "Control of a mobile robot for the push-a-box operation," in *Proc. of IEEE Intl. Conf. on Robotics and Automation*, Nice, France, May 1992, pp. 761–766.

[7] B. J. Thibodeau, P. Deegan, and R. Grupen, "Static analysis of contact forces with a mobile manipulator," in *Proc. of IEEE Intl. Conf. on Robotics and Autonomation*, Orlando, Florida, USA, May 2006, pp. 4007–4012.

[8] Y. Liu and G. Liu, "Track-stair interaction analysis and online tip-over prediction for a self-reconfigurable tracked mobile robot climbing stairs," *IEEE/ASME Trans. on Mechatronics, (in press)*, 2008.

[9] ——, "Track-stair and vehicle-manipulator interaction analysis for tracked mobile manipulators climbing stairs," in *Proc. of IEEE Intl. Conf. on Autom. Sci. and Eng.*, Washington DC, USA, Aug. 2008.

[10] ——, "Kinematics and interaction analysis for tracked mobile manipulators," in *Proc. IEEE/RSJ Intl. Conf. on Intelligent Robotics and Syst.*, San Diego, CA, USA, Oct 2007, pp. 267–272.

[11] Y. Yamamoto and X. Yun, "Effect of the dynamic interaction on coordinated control of mobile manipulators," *IEEE Trans. on Robotics and Automation*, vol. 12, no. 5, pp. 816–824, Oct. 1996.

[12] J. Y. Wong, *Theory of Ground Vehicles*, 4th ed. NJ, USA: John Wiley & Sons Inc., 2008.

[13] ESI, LMA series of mobile platforms. [Online]. Available: http://www.esit.com/mobileRobots.php